Whole-rock multivariate geochemical data sets of Carajás iron oxide copper-gold and hydrothermal nickel deposits: fingerprint and prediction of the hydrothermal zoning

Luiz Dutra[1], Lena Monteiro[1], Cleyton Carneiro[2], Rodrigo César Teixeira de Gouvêa[2], Lucas Brito[1]

[1]*Programa de Pós-Graduação em Recursos Minerais e Hidrogeologia, Instituto de Geociências, Universidade de São Paulo*

[2]*Integrações Tecnológicas em Análises de Rochas e Fluidos (InTRA), Escola Politécnica, Universidade de São Paulo*

Introduction

The magmatic-hydrothermal system is enveloped by alkali alteration zones, which reflect the ore-forming process such as fluid-rock interaction, fluid mixing and metal endowment being a powerful tool to vector towards ore zone in mineral exploration programs. The mineral paragenetic sequences, and hence the element associations, in the zonation patterns are mainly controlled by the superimposition of these geological and physicochemical changes during the system development (Montreuil et al., 2016a, 2016b; Dmitrijeva et al., 2019, 2022).

In this context, the whole-rock geochemical data from six drill holes of the GT-34 and Castanha deposits were used in multivariate analysis (e.g., **hierarchical clustering** - HC, **principal component analysis** - PCA, and **self-organizing maps** - SOM) to characterize the **chemical signature of mineralization** and **evaluate the predictive clustering** (data-driven decisions) **of the data to define the hydrothermal alteration zones** in the Southern Copper Belt in the Carajás Province (Figure 1).

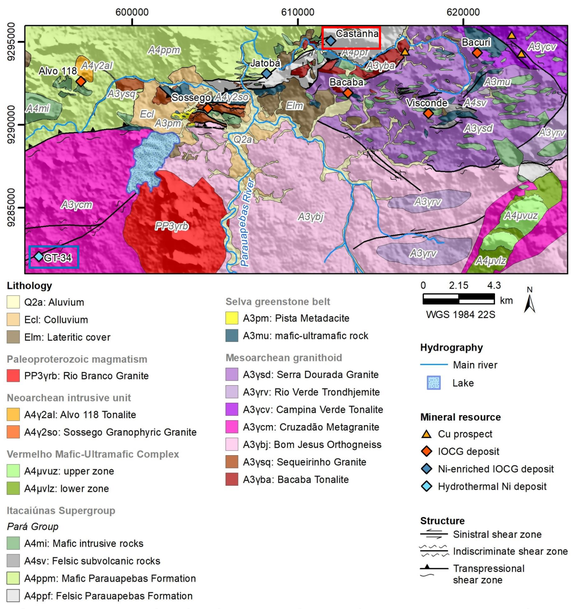

Figure 1. Geological map of Southern Copper Belt and locations of hydrothermal deposits.

Data and pre-processing

The whole-rock multi-element geochemical data were made available by Vale S.A. Assay data were collected from 1m-long samples along each drill core. The GT-34 deposit data presents 683 samples encompassing As, Co, Cr, Cu, F, Fe, Mg, Mn, Ni, P, Pb, Pd, Pt, S, Ti, V, Zn and Au, while the Castanha deposit database has 916 samples and is made of Ag, Au, Co, Cu, Mo, Ni, Pb and Zn. The pre-processing encompassed the replacing of the values below the minimum detection limit with half of the limit of detection of each element.

Multivariate statistical analyses

Hierarchical clustering (HC). The geochemical affinities in each deposit are shown as clusters in the HC dendrogram, where the height shows the relative distance between each group. The dendrogram shows that three groups were identified in the GT-34 deposit, which indicates that the mineralization, hosted in granitic and tonalitic rocks, presents a contribution of mafic-ultramafic sources or metals previously hosted in magmatic sulfides. Associations of (i) Ni reveal the mafic-ultramafic inheritance with Cr, Pt and Mn; (ii) Cu with Ti, Co, As, Fe and S; and (iii) Au with Pd and Pb. Fluids likely leached these elements with high fluorine fugacity (association of Au with F). The Castanha deposit has the typical IOCG geochemical signature from the SCB with the associations of Ag-Ni, Fe-Mn-As-Zn-Mo-Pb and Cu-Au-Co (Figure 2).

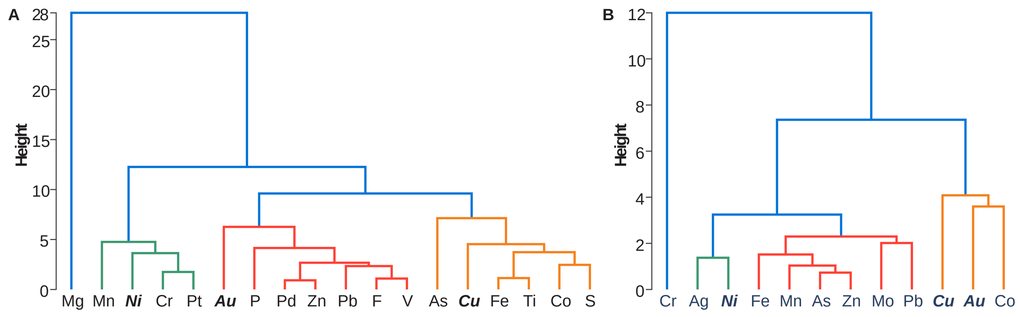

Figure 2. Hierarchical cluster dendrogram of GT-34 (A) and Castanha (B) deposit geochemical data.

Principal component analysis (PCA). We used PCA to inspect data and highlight the most relevant trends. The PCA aims to explain the maximum amount of data variance on orthogonal axes, ordered by the proportion of the data's explained variance (Silva et al., 2022).

The centered log-ratio (CLR) transformed data were used as the input value for the PCA. This transformation eliminates correlations among geochemical variables and moves the compositional data into Euclidian space (Zhou et al., 2018; Zhao et al., 2022). The PCA results indicate four associations for the GT-34 mineralization, where Fe-V-F-Mg-Ti, Au-Cr-Pt and P-Cu-Ni-S-Co occur on opposite sides of PC1 and Mn-Pb-As, Pd and Zn are lined up according to PC2. The Castanha data point to two distinct associations similar to the HC, Cu-Ni-Ag-Au-Co and Pb-Cr-Mn-Mo-Zn-Fe (Figure 3).

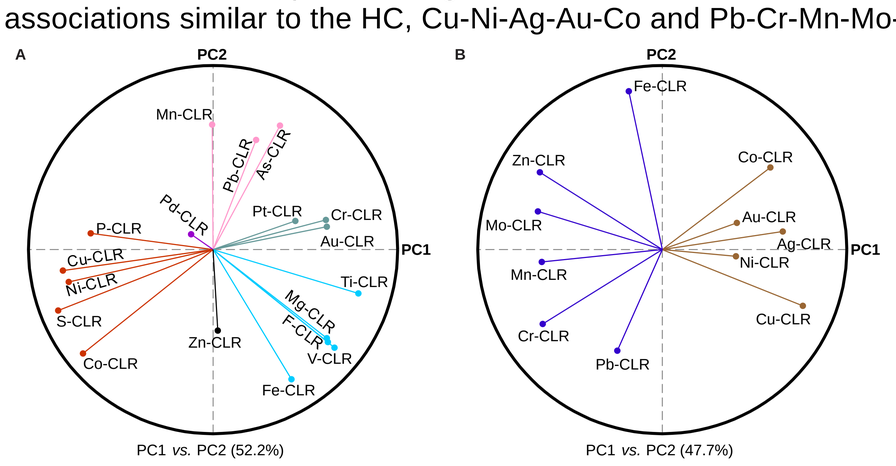

Figure 3. Hierarchical cluster dendrogram of GT-34 (A) and Castanha (B) deposit geochemical data.

Self-organizing maps (SOM). The SOM projects the multi-dimensional data into a lower-dimensional representation attempting to group the data subsets with similar characteristics into the same cluster. Therefore, the SOM can predict the geochemical signature of distinct rocks or hydrothermal alteration zones (Kohonen, 2001; Carneiro et al., 2012; Wu et al., 2021). The PCA is often used as a dimensionality reduction, and as our analysis showed, the five most important PCs (PC1 to PC5) can explain more than 80% of the variability of geochemistry data (Figure 4). Thus, these PCs were chosen as input parameters in the SOM to facilitate data clustering (Figure 5).

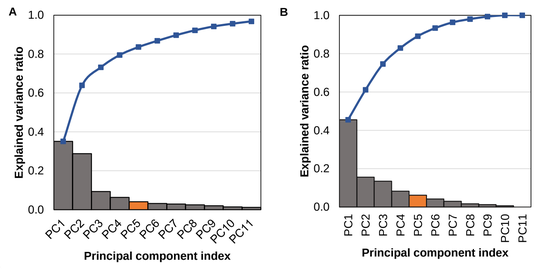

Figure 4. Explained variance ratios from principal component analysis of geochemical data of GT-34 (A) and Castanha (B) deposits.

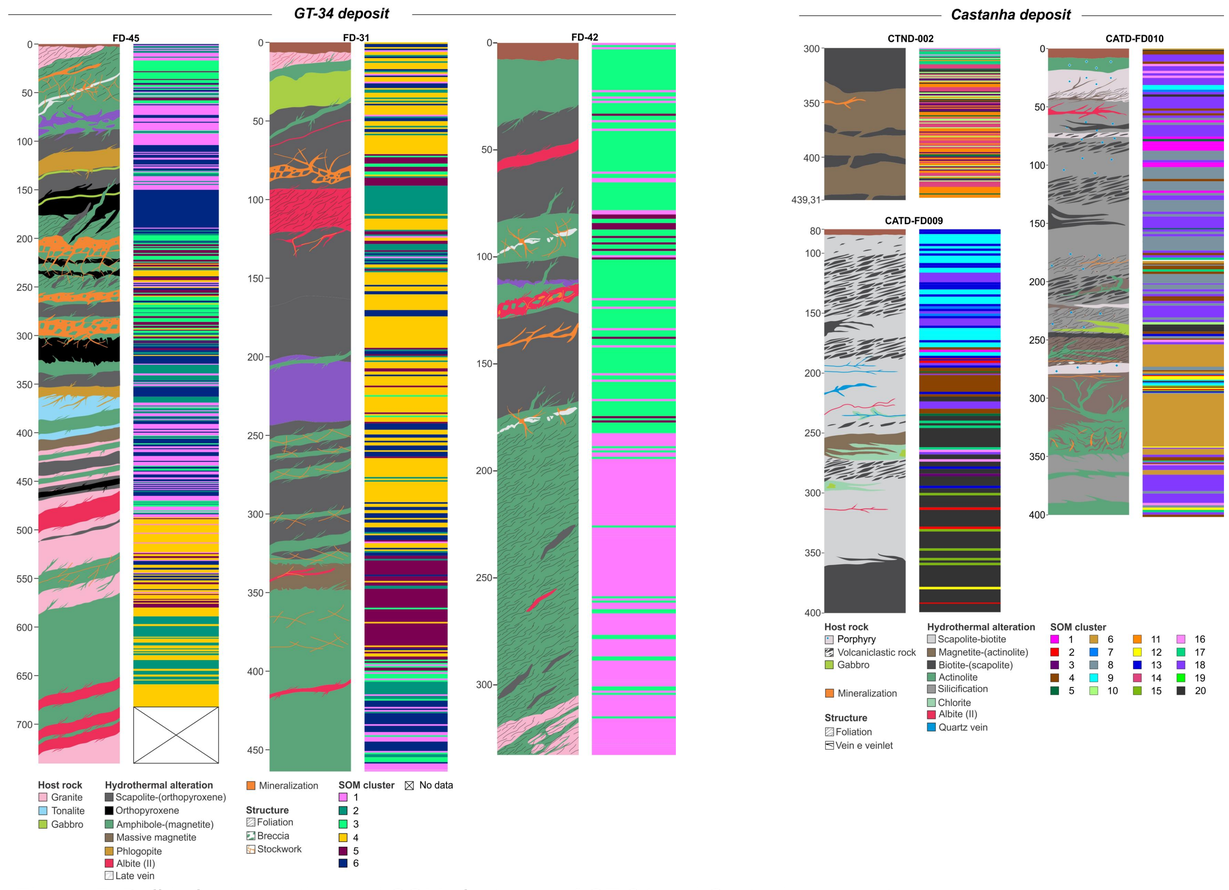

Figure 5. Drill hole description and SOM clustering of GT-34 and Castanha deposits.

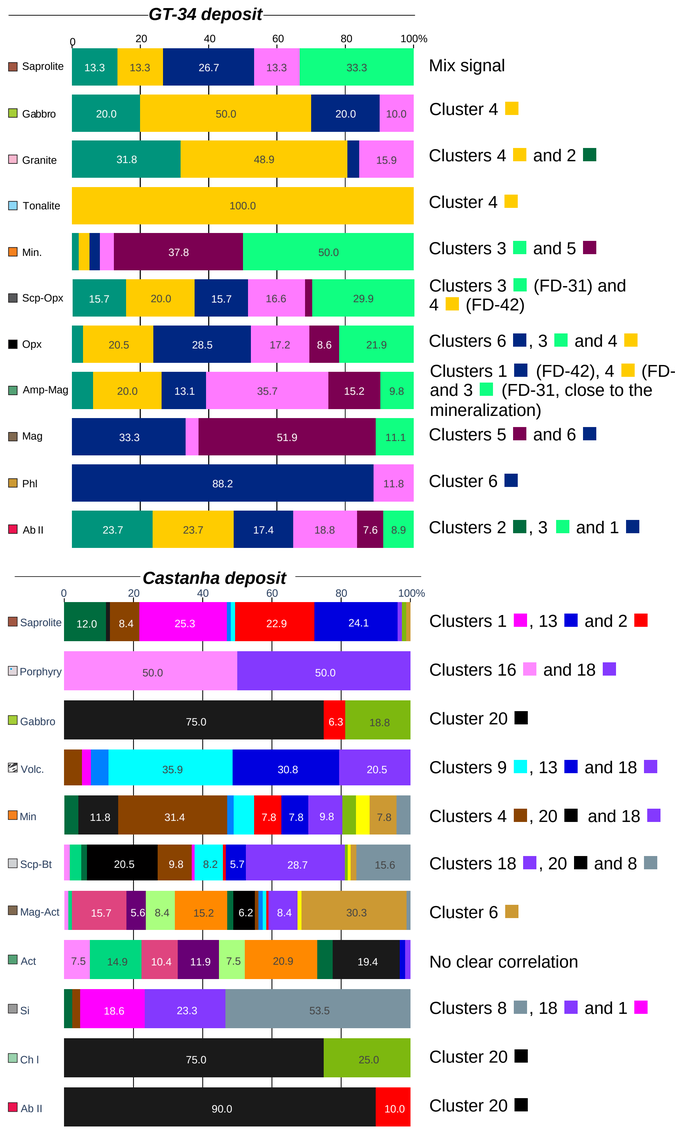

Figure 6. Correlation among host rock, alteration facies and SOM clustering of GT-34 and Castanha deposits.

Conclusion

The unsupervised multivariate analysis suggests that:

i. Mineralization and intense alteration zones in the GT-34 deposit likely reflect the element leaching from mafic-ultramafic rocks by F-rich fluid;
ii. The Castanha hydrothermal system has the typical IOCG geochemical signature from the SCB;
iii. The hydrothermal alterations in the GT-34 deposit differ from the host rocks by the greater matching with clusters 3, 5 and 6 (Figure 6). Notably, the alterations with orthopyroxene, magnetite and phlogopite present a better correlation with the clusters due to the intense replacement of minerals from previous hydrothermal alterations and the host rocks; and
iv. The hydrothermal alterations and mineralization in the Castanha deposit correlate with more than one cluster due to the frequent overlapping of alteration facies and the reduced number of elements in the database.

References

Carneiro, C. de C. et al. Geophysics 77, K17–K24 (2012), doi:10.1190/geo2011-0302.1
Dmitrijeva, M. et al. Econ. Geol. 117, 853–874 (2022), doi:10.5382/econgeo.4904
Dmitrijeva, M. et al. Ore Geol. Rev. 105, 86–101 (2019), doi:10.1016/j.oregeorev.2018.12.013
Kohonen, T. 30, (Springer Berlin Heidelberg, 2001), doi:10.1007/978-3-642-56927-2.
Montreuil, J. F. et al. Econ. Geol. 111, 2139–2168 (2016a), doi:10.2113/econgeo.111.8.2139
Montreuil, J. F. et al. Ore Geol. Rev. 72, 562–584 (2016b), doi:10.1016/j.oregeorev.2015.08.010
Silva, G. F. da et al. J. Geochemical Explor. 232, 106885 (2022), doi:10.1016/j.gexplo.2021.106885
Wu, G. et al. Nat. Resour. Res. 30, 1053–1068 (2021), doi:10.1007/s11053-020-09788-z
Zhao, Z. et al. Minerals 12, 1035 (2022), doi:10.3390/min12081035
Zhou, S. et al. Front. Earth Sci. 12, 491–505 (2018), doi:10.1007/s11707-017-0682-8

Acknowledge

The authors are grateful for the support of Vale, ADIMB and CAPES.

Contact: luizdutra@usp.br

RG: Luiz-Dutra-2 in: dutraluiz